Decoupling in the Similarity Renormalization Group for Nucleon-Nucleon Forces

E.D. Jurgenson [a], S.K. Bogner [a,b], R.J. Furnstahl [a], R.J. Perry [a]

[a] *Department of Physics, The Ohio State University, Columbus, OH 43210*

[b] *National Superconducting Cyclotron Laboratory and Department of Physics and Astronomy, Michigan State University, East Lansing, MI 48844*

Abstract

Decoupling via the Similarity Renormalization Group (SRG) of low-energy nuclear physics from high-energy details of the nucleon-nucleon interaction is examined for two-body observables and few-body binding energies. The universal nature of this decoupling is illustrated and errors from suppressing high-momentum modes above the decoupling scale are shown to be perturbatively small.

1 Introduction

The Similarity Renormalization Group (SRG) [1,2,3] provides a compelling method for evolving internucleon forces to softer forms [4,5]. While observables are unchanged by the SRG's unitary transformations, the contributions from high-momentum intermediate states to low-energy observables is modified by the running transformation. In particular, the SRG as implemented in Refs. [4,5] has the effect of partially diagonalizing the momentum-space potential to a width of order the evolution parameter. Because of this partial diagonalization, one anticipates a direct decoupling of low-energy observables from high-energy degrees of freedom.

In Ref. [5], evidence for decoupling at low momentum was shown for the Argonne V18 [6] potential in calculations of phase shifts and the deuteron. In this letter, we extend the demonstration of decoupling to nucleon-nucleon (NN) potentials from chiral effective field theory (EFT) [7,8] and to few-body

Email addresses: jurgenson.1@osu.edu (E.D. Jurgenson), bogner@nscl.msu.edu (S.K. Bogner), furnstahl.1@osu.edu (R.J. Furnstahl), perry@mps.ohio-state.edu (R.J. Perry).

nuclei up to $A = 6$ to verify its universal nature and to show quantitatively that the residual coupling is perturbative above the energy corresponding to the SRG evolution parameter. One might imagine that there is little to gain by evolving already-soft chiral EFT potentials to lower momentum, but recent work shows significant advantages for the nuclear few- and many-body problem [9]. This is consistent with the additional decoupling we find here.

The practical test for decoupling is whether changing high-momentum matrix elements of the potential changes low-energy observables. Our strategy is to first evolve the initial potential $V_{\rm NN}$ with the SRG equations to obtain the SRG potential V_s, where s denotes the flow parameter of the transformation. Then we apply a parametrized regulator to cut off the high-momentum part of the evolved potential in a controlled way. This cutoff potential is used to calculate few-body observables and their relative errors. By varying the parameters of the regulator and correlating them with errors in the calculated observables, we have a diagnostic tool to quantitatively analyze the decoupling.

In Section 2, we give background on decoupling in the SRG and the use of a smooth regulator to quantify decoupling. In Section 3, we analyze the relative error between phase shifts calculated with uncut and cut potentials and find a clean power law dependence at larger momenta that follows from perturbation theory. In Section 4, we examine observables for the deuteron bound state and find the same perturbative behavior for the errors. Using the No-Core Shell Model (NCSM) [10,11,12,13,14], we verify this behavior for few-body calculations in Section 5 and summarize in Section 6.

2 Decoupling in the SRG

As in Ref. [4], we apply the similarity renormalization group (SRG) transformations to NN interactions based on the flow equation formalism of Wegner [2]. The evolution or flow of the Hamiltonian with a parameter s is a series of unitary transformations,

$$H_s = U_s H U_s^\dagger \equiv T_{\rm rel} + V_s \ , \tag{1}$$

where $T_{\rm rel}$ is the relative kinetic energy and $H = T_{\rm rel} + V$ is the initial Hamiltonian in the center-of-mass system. Equation (1) defines the evolved potential V_s, with $T_{\rm rel}$ taken to be independent of s. Then H_s evolves according to

$$\frac{dH_s}{ds} = [\eta_s, H_s] \ , \tag{2}$$

with

$$\eta_s = \frac{dU_s}{ds} U_s^\dagger = -\eta_s^\dagger \ . \tag{3}$$

Choosing η_s specifies the transformation, which is taken as the commutator of an operator, G_s, with the Hamiltonian,

$$\eta(s) = [G_s, H_s] \ , \tag{4}$$

so that

$$\frac{dH_s}{ds} = [[G_s, H_s], H_s] \ . \tag{5}$$

Applications to nuclear physics to date in a partial-wave momentum basis have used $G_s = T_{\rm rel}$ [4], but one could also use momentum-diagonal operators such as $T^2_{\rm rel}$, $T^3_{\rm rel}$, or the running diagonal Hamiltonian H_D, as advocated by Wegner [2].

The source of decoupling is the partial diagonalization of the Hamiltonian by the SRG evolution. For the NN interaction, the flow equation (5) can be simply evaluated in the space of discretized relative momentum NN states [4]. For a given partial wave, with units where $\hbar^2/M = 1$, we define diagonal matrix elements of momentum k as

$$\langle k|H_s|k\rangle = \langle k|H_D|k\rangle \equiv e_k \ , \tag{6}$$

and

$$\langle k|T_{\rm rel}|k\rangle \equiv \epsilon_k = k^2 \ . \tag{7}$$

With Wegner's choice, $G_s = H_D$, the flow equation for each matrix element is

$$\frac{d}{ds}\langle k|H_s|k'\rangle = \sum_q (e_k + e_{k'} - 2e_q)\langle k|H_s|q\rangle\langle q|H_s|k'\rangle \ . \tag{8}$$

By considering the trace of H_s^2, one can show that off-diagonal matrix elements as a whole decrease in magnitude unless there are energy degeneracies [2].

If we take $G_s = T_{\rm rel}$, the flow equation for each matrix element is

$$\begin{aligned}\frac{d}{ds}\langle k|H_s|k'\rangle &= \sum_q (\epsilon_k + \epsilon_{k'} - 2\epsilon_q)\langle k|H_s|q\rangle\langle q|H_s|k'\rangle \\ &= -(\epsilon_k - \epsilon_{k'})^2\langle k|V_s|k'\rangle \\ &\quad + \sum_q (\epsilon_k + \epsilon_{k'} - 2\epsilon_q)\langle k|V_s|q\rangle\langle q|V_s|k'\rangle \ .\end{aligned} \tag{9}$$

In this case, it can be shown that off-diagonal elements are not guaranteed to decrease monotonically if $e_k - e_{k'}$ and $\epsilon_k - \epsilon_{k'}$ have opposite signs (see Ref. [15] for details). However, this does not happen in the range of s that has been considered in the nuclear case because of the dominance of the kinetic energy.

This dominance can be used to find a semi-quantitative approximation for the flow of off-diagonal matrix elements by keeping only the first term on the right

side of Eq. (9) (or, equivalently, substituting $\langle k|H_s|q\rangle \to \epsilon_k\,\delta_{kq}$). Then the flow equation applied to individual off-diagonal matrix elements simplifies to

$$\frac{d}{ds}\langle k|H_s|k'\rangle = \frac{d}{ds}\langle k|V_s|k'\rangle \approx -(\epsilon_k - \epsilon_{k'})^2\,\langle k|V_s|k'\rangle\ , \tag{10}$$

which has the simple exponential solution

$$\langle k|V_s|k'\rangle \approx \langle k|V_{s=0}|k'\rangle e^{-s(\epsilon_k-\epsilon_{k'})^2}\ . \tag{11}$$

In Fig. 1, we plot $\langle k|V_s|k'\rangle \approx \langle k|V_{s=0}|k'\rangle$ and the approximation from Eq. (11) versus s for some representative off-diagonal points in two partial waves. In almost all cases the approximation gives a reasonable estimate of the monotonic decrease to zero; in the one exception there is a significantly more rapid decrease than predicted.

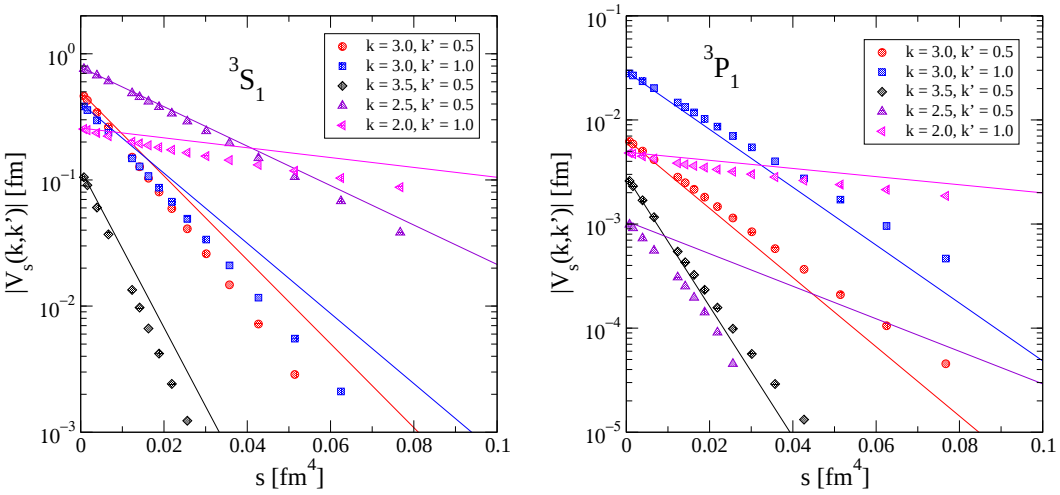

Fig. 1. Absolute value of the matrix element $\langle k|V_s|k'\rangle$ for a representative sampling of off-diagonal (k,k') pairs as a function of s, compared with the simple solutions from Eq. (11), which are straight lines (they agree at $s=0$). Two partial waves are shown.

It is convenient to switch to the flow variable $\lambda = 1/s^{1/4}$, which has units of fm^{-1}, since Eq. (11) shows that λ is a measure of the resulting diagonal width of V_s in momentum space. More precisely, the matrix $\langle k|V_s|k'\rangle$ plotted as a function of kinetic energies k^2 and k'^2 will rapidly go to zero outside of a diagonal band roughly of width λ^2, which is verified by numerical calculations [16]. For momenta within λ of the diagonal, the omitted quadratic part of the flow equation is, of course, essential, and drives the flow of physics information necessary to preserve unitarity.

The tool we will use to study decoupling is a smooth exponential regulator applied to the potential to cut off momenta above Λ:

$$V_{\lambda,\Lambda}(k,k') = e^{-(k^2/\Lambda^2)^n}V_\lambda(k,k')e^{-(k'^2/\Lambda^2)^n}\ , \tag{12}$$

where n takes on integer values. From the cut potentials we calculate observables such as phase shifts and ground-state energies and compare to values calculated with the corresponding uncut potential. If there is decoupling between matrix elements in a given potential (evolved or otherwise), we should be able to set those elements to zero in this systematic way and use the relative error in the observable as a metric of the degree of decoupling. By varying n we can identify quantitatively the residual coupling strength.

The SRG transformations used here are truncated at the two-body level, which means that they are only approximately unitary for $A > 3$ and observables will vary with s. In these cases decoupling is tested by comparing cut to uncut potentials at a fixed s. All two-body observables calculated with the uncut H_s are independent of s to within numerical precision. The actual numerical error depends on the details of the discretization (e.g., the number and distribution of mesh points, usually gaussian) and on the accuracy and tolerances of the differential equation solver. While in practice we can make such errors very small, to avoid mixing up small errors we will also compare cut to uncut potentials rather than to the unevolved ($s = 0$) potential for two-body observables.

3 Phase Shift Errors

In the upper-left panel of Fig. 2, we show results for the $^1S_0$ phase shifts vs. energy calculated using the unevolved 500 MeV N^{3}LO potential of Ref. [7] and the corresponding SRG potential evolved to $\lambda = 2.0\,\mathrm{fm}^{-1}$ and then cut using the regulator of Eq. (12) with $n = 8$. We do not explicitly show results from uncut SRG potentials, because they are indistinguishable from the unevolved results.

The qualitative pattern is that when the regulator parameter Λ is greater than λ, there is good agreement of phase shifts from uncut and cut potentials at small energies and reasonable agreement up to the energy corresponding to the momentum of the cut, $E_{\mathrm{lab}} \approx 2\Lambda^2/m$ (with $\hbar = 1$). When V_{srg} is cut below λ, there is poor agreement everywhere and the phase shift is zero above this energy (e.g., above $E_{\mathrm{lab}} = 100\,\mathrm{MeV}$ for $\Lambda = 1.1\,\mathrm{fm}^{-1}$). Thus the decoupling of high and low momentum means that we can explicitly cut out the high-momentum part of the evolved potential without significantly distorting low-energy phase shifts as long as we don't cut below λ. Cutting out the high-momentum part of conventional nuclear potentials *does* cause distortions, which has led to the misconception that reproducing high-energy phase shifts is important for low-energy nuclear structure observables [5].

The quantitative systematics of SRG decoupling is documented in the other

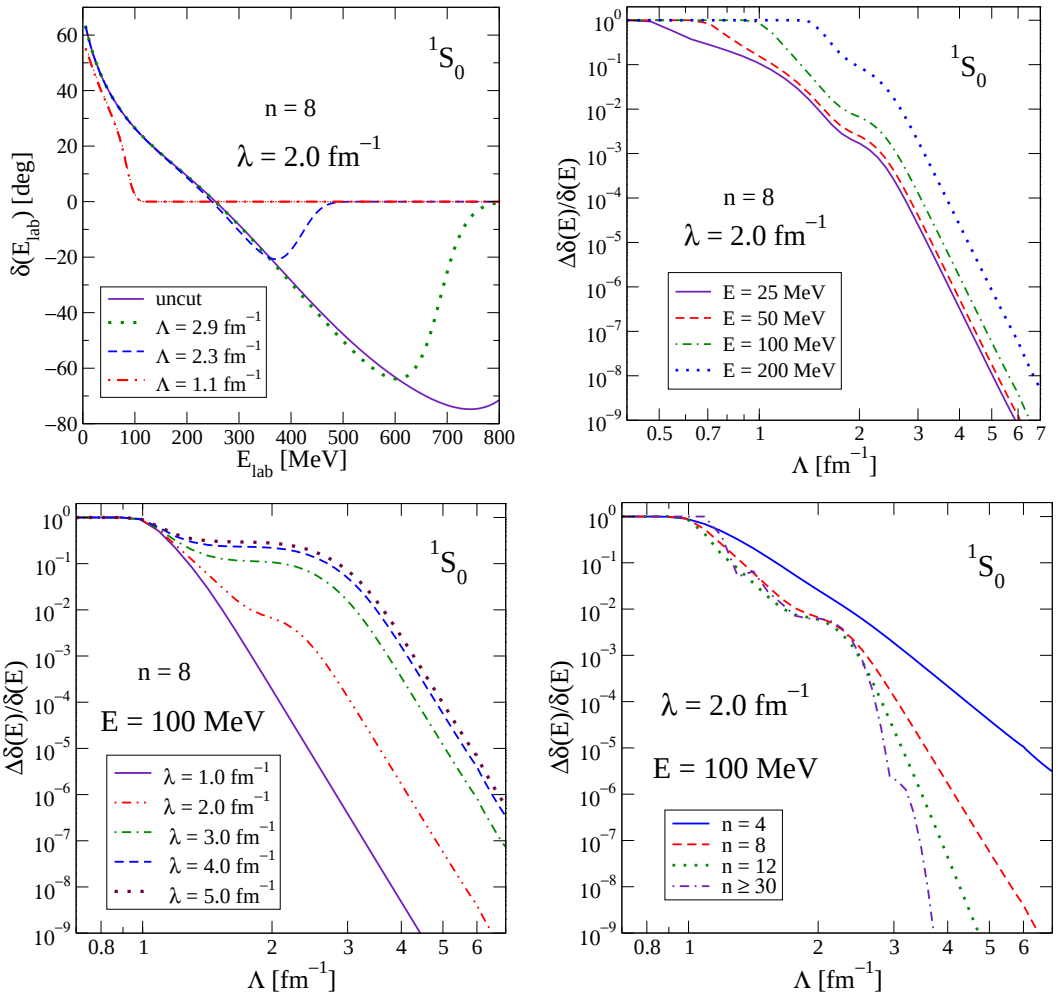

Fig. 2. Phase shifts and relative errors in the $^1S_0$ channel for SRG potentials evolved from the N^{3}LO (500 MeV) potential of Ref. [7]. The upper-left graph shows the phase shifts vs. energy for the uncut $\lambda = 2\,\mathrm{fm}^{-1}$ potential and several cut versions with $n = 8$. The other panels show the relative error as a function of the momentum cut parameter Λ at various energies E, λ's, and n's, respectively.

panels of Fig. 2, where we look at the relative error as a function of the cutting momentum using log-log plots. In these error plots, three main regions are evident. In the region below the Λ corresponding to the fixed energy, the predicted phase shift goes to zero since the potential has vanishing matrix elements, so that the relative error goes to one. Starting at Λ slightly above the value of λ, there is a clear power-law decrease in the error. In between is a transition region without a definite pattern.

We focus here on the power-law region. In the lower-left pane, we find that this decoupling starts with a shoulder at momenta slightly above λ. This effect saturates when λ becomes comparable to the underlying cutoff of the original potential. In the upper-right pane we see that the shoulder signaling the start of the power-law decrease is not affected by the energy, E. This holds for other

values of λ and n. In the lower-right pane we vary the exponent of the regulator, n, which changes the smoothness of the regulator. The smoothness affects the slope of the power law and the fine details in the intermediate region, but does not change the position of the shoulder near λ. As discussed below, the power-law behavior in the relative error signifies perturbative decoupling with a strength given by the sharpness of the regulator used to cut off the potential.

We checked this decoupling behavior in different partial waves and for other N^{3}LO potentials and found the same perturbative region in all cases. Representative partial waves are shown for various λ values in Fig. 3. The potential in the S waves typically passes through zero for momenta in the region of $\lambda = 2\,\mathrm{fm}^{-1}$ (see, for example, Ref. [16]), which might lead one to associate decoupling with this structure. The error plots for other partial waves that lack this structure show that it is a more general consequence of the SRG evolution.

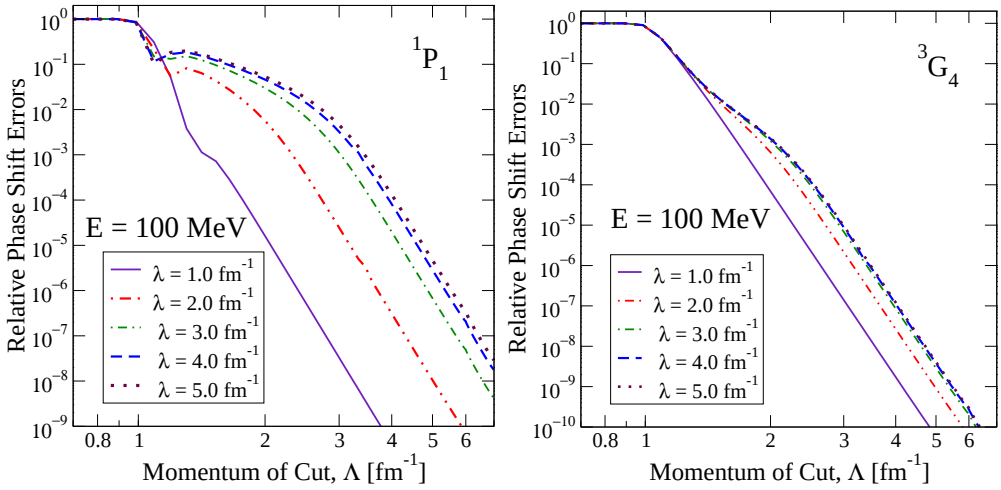

Fig. 3. The phase shift errors computed in select partial waves, using a regulator with $n = 8$. Other channels exhibit the same power-law dependence of the error for $\Lambda > \lambda$.

Indeed, the behavior of the errors in the decoupling region, where $\Lambda > \lambda$, can be directly understood as a consequence of the partial diagonalization of the evolved potential. The calculation of the phase shift at a low-energy $k^2 \ll \lambda^2$ will involve an integral over p of $V_{\lambda,\Lambda}(k,p)$. But the potential cuts off the integral at roughly $p^2 \approx k^2 + \lambda^2 < \Lambda^2$, which means that we can expand the difference in the uncut and cut potentials:

$$\delta V_{\lambda,\Lambda}(k,p) \equiv V_\lambda(k,p) - V_{\lambda,\Lambda}(k,p) \approx \left(\frac{k^{2n}}{\Lambda^{2n}} + \frac{p^{2n}}{\Lambda^{2n}}\right) V(k,p)\ . \qquad (13)$$

Simple perturbation theory in δV then predicts the dependence of the phase shift error to be $1/\Lambda^{2n}$, which is the power-law dependence seen in Figs. 2 and 3. The accuracy of first-order perturbation theory is evidenced by the constant

slope of the error curves, which translates into perturbatively small residual coupling.

The detailed dependence on the energy and λ is not so trivially extracted. However, the weak dependence on $E_{\rm lab} \leq 100\,{\rm MeV}$ and strong dependence on $\lambda < 3\,{\rm fm}^{-1}$ at fixed Λ seen in Fig. 2 implies that the integration picks up the scale λ, so that the dominant error scales as $(\lambda/\Lambda)^{2n}$. This is, in fact, observed numerically for intermediate values of λ (e.g., for $1.8\,{\rm fm}^{-1} < \lambda < 2.8\,{\rm fm}^{-1}$ when $\Lambda = 3\,{\rm fm}^{-1}$).

4 Decoupling and Deuteron Observables

To test the generality of the observations made for phase shifts, the same techniques were applied to other low-energy observables such as the deuteron binding energy, radius, and quadrupole moment. The binding energy and momentum-space wavefunction were computed using standard eigenvalue methods. The computation of Q_d and r_d from the wavefunction uses [17],

$$Q_d = -\frac{1}{20}\int_0^\infty dk \left[\sqrt{8}\left(k^2\,\frac{d\widetilde{u}(k)}{dk}\frac{d\widetilde{w}(k)}{dk} + 3k\,\widetilde{w}(k)\frac{d\widetilde{u}(k)}{dk}\right) + k^2\left(\frac{d\widetilde{w}(k)}{dk}\right)^2 + 6\,\widetilde{w}(k)^2\right], \tag{14}$$

and

$$r_d = \frac{1}{2}\left[\int_0^\infty dk \left\{\left(k\,\frac{d\widetilde{u}(k)}{dk}\right)^2 + \left(k\,\frac{d\widetilde{w}(k)}{dk}\right)^2 + 6\,\widetilde{w}(k)^2\right\}\right]^{1/2}, \tag{15}$$

where $\widetilde{u}(k)$ and $\widetilde{w}(k)$ correspond to the S and D components of the deuteron wavefunction respectively. We again computed relative errors in these observables and, as shown in Fig. 4 for the energy and radius, the errors show the same behavior as observed for the phase shifts. That is, a power-law drop-off in the error begins at Λ just above λ, with a slope determined by the sharpness of the regulator as given by n. The relative error for the quadrupole moment is not shown but is very similar to that for the radius.

As with the phase shift, the analytic dependence of the error from cutting the potential can be estimated directly in perturbation theory. In this case, partial diagonalization of the potential means that the deuteron wave function has negligible momentum components starting slightly above λ. This in turn validates the expansion in Eq. (13) and the dependence of the errors on $1/\Lambda^{2n}$. The numerical calculation of the error in perturbation theory is plotted in Fig. 4 and shows close agreement in the decoupling region $\Lambda > \lambda$.

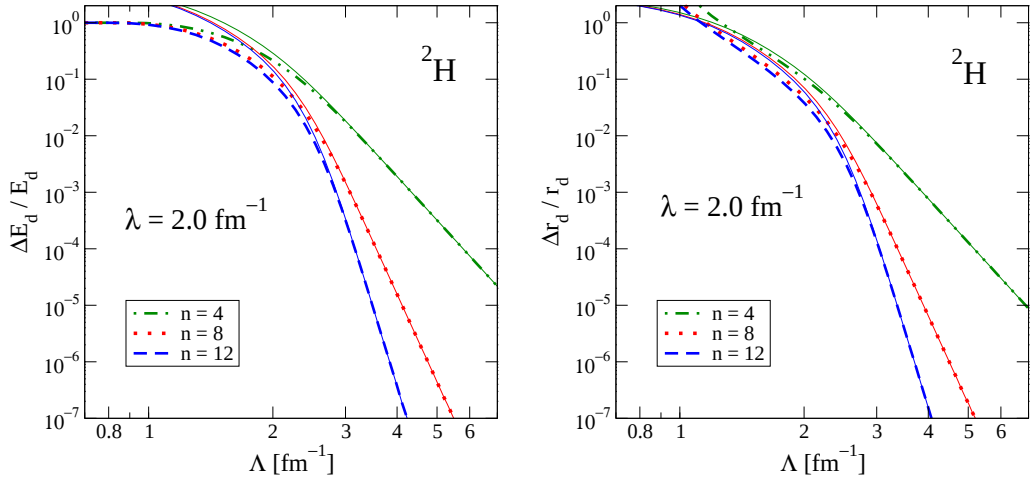

Fig. 4. The relative error vs. cut parameter Λ of the deuteron energy (left) and rms radius (right) with several values of the regulator parameter n indicated in the legends. In each case, the near-by solid line is the estimate of the error using first-order perturbation theory with Eq. (13).

5 Decoupling and Few-Body Energies with the NCSM

The calculations described above have been only for two-particle systems. Using NCSM calculations of ground-state energies with the Many-Fermion Dynamics (MFD) code [18], we can test whether the high-energy decoupling behavior extends to few-body systems. In the present study, only NN interactions were considered, with the testing of decoupling with many-body forces deferred to a future investigation. However, we note that the general features of the SRG exhibited in Section 2 implies that off-diagonal matrix elements (with respect to energy) of the three-body force will be suppressed, with decoupling as an expected consequence.

We first verified that the decoupling behavior already observed using a direct calculation of the deuteron wavefunction is reproduced using the MFD. We then calculated a series of larger nuclei, including ^{3}H, ^{4}He, and ^{6}Li, comparing results from uncut and a range of cut potentials evolved to different values of λ. On the left panel of Fig. 5, the ^{4}He ground-state energy is plotted versus the regulator parameter Λ for several different values of the SRG flow parameter λ. Each of the plotted points is at a basis size $N_{\max} = 12$; this is within several hundred keV of the energy from extrapolating to $N_{\max} = \infty$. A similar plot for ^{6}Li is given in the left panel of Fig. 6 using a basis size $N_{\max} = 8$, which is within several hundred keV of the extrapolated energy for $\lambda = 1.5\,\mathrm{fm}^{-1}$ but still several MeV off for $\lambda = 3.0\,\mathrm{fm}^{-1}$. The uncut ($\Lambda \to \infty$) energies vary for each λ because the SRG evolution includes the NN interaction only; the closeness of the results for $\lambda = 2\,\mathrm{fm}^{-1}$ and $3\,\mathrm{fm}^{-1}$ for ^{4}He is accidential (see Ref. [9] for further discussion about the running of the energies).

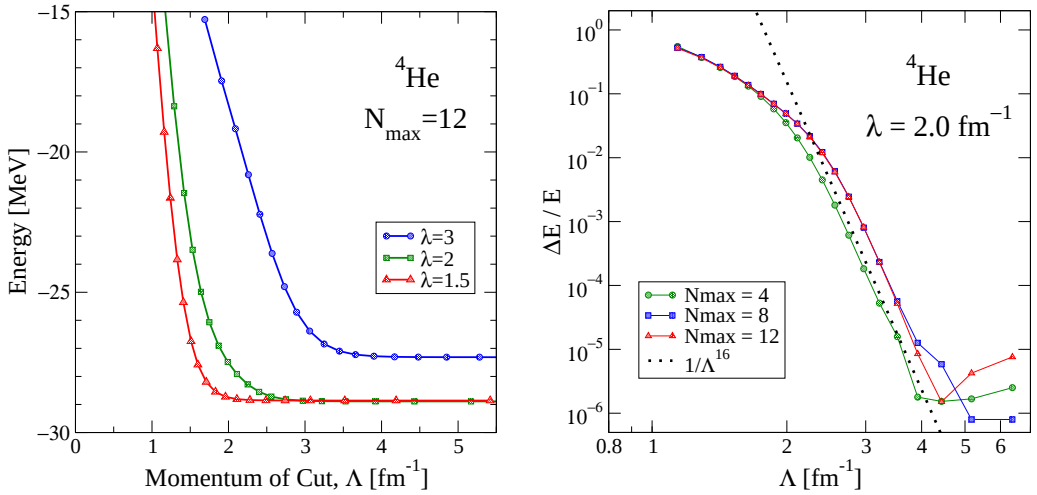

Fig. 5. Calculations of the ^{4}He ground-state energy using the NCSM. On the left is the energy obtained from the NCSM for potentials evolved to several different λ values as a function of the cut (regulator) momentum Λ with $n = 8$. On the right is the relative error of the energy for the $\lambda = 2\,\mathrm{fm}^{-1}$ case as a function of the cut momentum (with $n = 8$) for several different harmonic oscillator basis sizes. Also shown is the slope of the error in the decoupling region predicted from perturbation theory (dotted line).

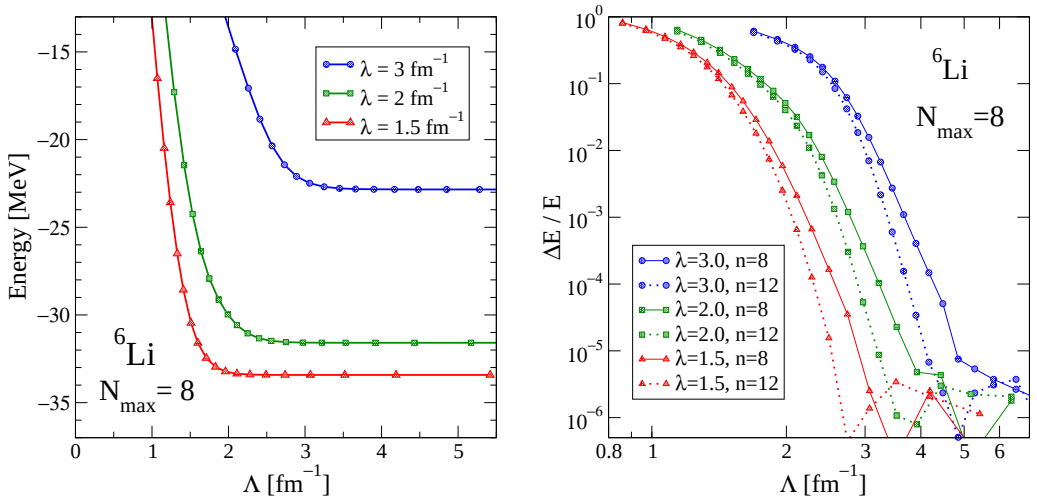

Fig. 6. Calculations of the ^{6}Li ground-state energy using the NCSM. On the left is the energy obtained from the NCSM for potentials evolved to several different λ values as a function of the cut (regulator) momentum Λ with $n = 8$. On the right is the relative error of the energy for the same λ's as a function of the cut momentum for the same λ values but with two values of n.

Both examples show that when the potential is cut with Λ comparable to λ or lower, the converged energy is significantly different from the asymptotic uncut value, while it approaches that value rapidly as Λ moves above λ. This means that, for smaller λ, more high momentum matrix elements can be discarded without a loss of accuracy. This decoupling explains the greatly improved

convergence with basis size seen in the NCSM for corresponding λ values [9].

The quantitative behavior of the relative error parallels that observed for two-body observables, as seen on the right panels of Figs. 5 and 6. In all cases, for a fixed value of λ the power decrease in the error starting with Λ slightly above λ is clearly seen, even though there are fewer digits of precision in the NCSM results (so the relative error is in the range 10^{-6}–10^{-5} at best). The same perturbative residual coupling is seen for different basis sizes, with the slope given by the dependence $1/\Lambda^{2n}$, although the onset of the decoupling region shifts to higher Λ until the calculation is near convergence (see Fig. 5). Similar results are found for other nuclei and for other values of λ.

We repeated the calculations with other choices of the SRG generator, G_s including $T_{\rm rel}^2$ and $H_{\rm D} = T_{\rm rel} + V_{\rm D}$, where $V_{\rm D}$ is the (running) diagonal part of the bare potential. We found that these other choices for G_s do not alter the power-law behavior region of the previous error plots. This provides further evidence that the high- and low-energy decoupling results primarily from the partially diagonalized nature of the evolved potential.

6 Summary

The evolution of nucleon-nucleon potentials with the Similarity Renormalization Group decouples high-energy degrees of freedom from calculations of low-energy observables. By using a steep but smooth exponential function of the form $\exp[-(k^2/\Lambda^2)^n]$ with integer n to set interaction matrix elements with relative momenta above Λ smoothly to zero, we have found that the residual coupling follows a clear and universal behavior. Decoupling is achieved for Λ above λ, the flow parameter for the SRG. The dependence on n was used to study the region of weak residual coupling, which was found to follow a power law predicted by leading-order perturbation theory. These results were shown to apply to NN phase shifts, several deuteron observables, and the ground-state energy of nuclei up to $A = 6$. Similar results are also found for other generators that are diagonal in momentum space.

We emphasize that the regulator used here was only a tool for studying the effect of the SRG on the potential. No cuts of this nature have been used or are proposed for calculations with NN potentials. However, the most important next step with the SRG is the evolution of three-body forces [19], which have significantly larger computational requirements. There is every indication that the SRG will induce the same decoupling for interactions that include three-body forces. These potentials will be projected on a momentum basis ordered by the kinetic energy of the states, and the SRG evolution equations will suppress matrix elements that are off-diagonal in that energy

basis [19]. Decoupling as observed here would allow a three-body computation to freeze irrelevant high-energy details during the evolution in a controlled way, which could significantly reduce the computational resources needed.

Acknowledgements

This work was supported in part by the National Science Foundation under Grant Grant Nos. PHY–0354916 and PHY–0653312, and the the UNEDF SciDAC Collaboration under DOE Grant DE-FC02-07ER41457.

References

[1] S.D. Glazek and K.G. Wilson, Phys. Rev. D **48** (1993) 5863; Phys. Rev. D **49** (1994) 4214.

[2] F. Wegner, Ann. Phys. (Leipzig) **3** (1994) 77; Phys. Rep. **348** (2001) 77.

[3] J. Kehrein, *The Flow Equation Approach to Many-Particle Systems* (Springer, Berlin, 2006).

[4] S.K. Bogner, R.J. Furnstahl, and R.J. Perry, Phys. Rev. C **75** (2007) 061001.

[5] S.K. Bogner, R.J. Furnstahl, R.J. Perry, and A. Schwenk, Phys. Lett. B **649** (2007) 488.

[6] R.B. Wiringa, V.G.J. Stoks and R. Schiavilla, Phys. Rev. C **51** (1995) 38.

[7] D.R. Entem and R. Machleidt, Phys. Rev. C **68** (2003) 041001(R).

[8] E. Epelbaum, W. Glöckle and U.G. Meißner, Nucl. Phys. **A747** (2005) 362.

[9] S.K. Bogner, R.J. Furnstahl, P. Maris, R.J. Perry, A. Schwenk and J.P. Vary, arXiv:0708.3754 [nucl-th].

[10] P. Navrátil, J.P. Vary and B.R. Barrett, Phys. Rev. Lett. **84** (2000) 5728; Phys. Rev. C **62** (2000) 054311.

[11] P. Navrátil and W.E. Ormand, Phys. Rev. Lett. **88** (2002) 152502.

[12] P. Navrátil and W.E. Ormand, Phys. Rev. C **68** (2003) 034305.

[13] A. Nogga, P. Navrátil, B.R. Barrett and J.P. Vary, Phys. Rev. C **73** (2006) 064002.

[14] P. Navrátil, V.G. Gueorguiev, J.P. Vary, W.E. Ormand and A. Nogga, Phys. Rev. Lett. **99** (2007) 042501.

[15] S.D. Glazek and R.J. Perry, *The impact of bound states on similarity renormalization group transformations*; in preparation.

[16] See http://www.physics.ohio-state.edu/∼ntg/srg/ for documentary examples.

[17] S.K. Bogner, R.J. Furnstahl, S. Ramanan and A. Schwenk, Nucl. Phys. A **784**, 79 (2007).

[18] J.P. Vary, The Many-Fermion Dynamics Shell-Model Code, Iowa State University (1992) (unpublished); J.P. Vary and D.C. Zheng, ibid., (1994) (unpublished).

[19] S. K. Bogner, R. J. Furnstahl and R. J. Perry, arXiv:0708.1602 [nucl-th].